Molecular Catalysis 444 (2018) 53–61

Contents lists available at ScienceDirect

Molecular Catalysis

journal homepage: www.elsevier.com/locate/mcat

Research paper

Selective hydrogenation of benzoic acid to cyclohexane carboxylic acid over microwave-activated Ni/carbon catalysts

X.H. Lu[a,b,c], Y. Shen[a,b,c], J. He[a,c], R. Jing[a,c], P.P. Tao[a,c], A. Hu[a,c], R.F. Nie[a,c], D. Zhou[a,c], Q.H. Xia[a,c,*]

[a] Hubei Collaborative Innovation Center for Advanced Organic Chemical Materials, Hubei University, Wuhan 430062, PR China
[b] Hubei Key Laboratory for Processing and Application of Catalytic Materials, Huanggang Normal University, Huanggang 438000, PR China
[c] Ministry-of-Education Key Laboratory for the Synthesis and Application of Organic Functional Molecules, Hubei University, Wuhan 430062, PR China

ARTICLE INFO

Article history:
Received 21 July 2017
Received in revised form 2 October 2017
Accepted 10 October 2017

Keywords:
Selective hydrogenation
Benzoic acid
Cyclohexane carboxylic acids
Ni/carbon catalysts

ABSTRACT

High yields of cyclohexane carboxylic acids were obtained by direct hydrogenation of aromatic carboxylic acids over different Ni/carbon catalysts having distinctive surface properties. The catalysts were characterized by SEM, TEM, H_2-TPR and N_2 adsorption isotherms for the determination of BET surface area and porosity. The hydrogenation reaction was carried out in batch pressure reactor in gas-liquid phase at 200 °C. High selectivity (100%) of cyclohexane carboxylic acids at 86.2 mol% conversion of benzoic acid was achieved over microwave-activated biochar supported non-precious metal Ni catalyst. The 10%Ni/CSC-b catalyst has been investigated for hydrogenation of benzoic acid to cyclohexane carboxylic acids and shown little deactivation in stability test. The effects of Ni loading, high dispersion of Ni species, appropriate power of microwave heating and strong interaction of Ni species with carbon are of benefit to the reaction.

1. Introduction

Catalytic hydrogenation is an ubiquitous reaction and is used for instance in the synthesis of fine chemicals and fuel upgrading [1–5]. Increasing sustainability demands are now appealed for chemical production to improve catalytic selectivity, to minimize byproduct formation, to circumvent separation/purification operations and to avoid costly clean-up and disposal. Benzoic acid is an inexpensive feedstock [1] that can be hydrogenated to benzaldehyde [6–10], benzyl alcohol [11–13] or cyclohexane carboxylic acid [14–17] as important commercial products. The chemoselective hydrogenation of benzoic acids (BA) to cyclohexane carboxylic acid (CCA) is the most important reaction in the synthesis of caprolactam from toluene, and CCA is also an important organic intermediate for the synthesis of pharmaceutical industries for example praziquantel and ansatrienin [18–20]. So chemoselective hydrogenation of BA to CCA has attracted great interest all over the world [21–24].

The catalytic hydrogenation of carboxylic acids is performed industrially by using heterogeneous catalysts, such as noble metal catalysts, including Pd/C, Rh/C, PdxRuy, RuPt and platinum nanowire [25–27], have been widely applied in this transformation, and all exhibit high activities. Due to stability and can be used multiple times, heterogeneous catalysts are the preferred options for most processes in chemical industry [28,29]. In principle, in the case of the supported catalysts, two basic but important issues should be taken into account in order to design and screen suitable supports for catalytic applications. One of which is that the support must show high stability and high surface area; the other is that the support should contain high density of defect sites. There are a variety of materials that suitable as supports [30,31], among which carbons (including activated carbon [32], graphene [33] and carbon nanotubes [34]) are the most frequently used. As carbon materials are mainly composed of carbon and even can be made directly out of biomass, they are obviously "sustainable" support materials for Pd nanoparticles (NPs). However, the agglomeration and leaching of noble metal nanoparticles (such as Pd, Pt, Au) in the catalysts cannot be effectively avoided by simply treating the support using reagents such as nitric acid and hydrogen peroxide due to the weak interaction of surface oxygen groups [35], and also the high price of noble metal catalysts has limited their further application in industry.

Cyclohexanecarboxylic acid is an important organic synthesis intermediate, which itself is a good light curing agent, but also for the synthesis of the drug antiemulsion 392 and praziquantel (treatment of schistosomiasis), its derivatives such as cyclohexyl-

* Corresponding author at: Hubei Collaborative Innovation Center for Advanced Organic Chemical Materials, Hubei University, Wuhan 430062, PR China.
E-mail addresses: xia1965@yahoo.com, xiaqh518@aliyun.com (Q.H. Xia).

http://dx.doi.org/10.1016/j.mcat.2017.10.015
2468-8231/

methyl carbamate and *trans*-4-isopropylcyclohexyl acid are the important intermediates for the synthesis of many chemical products and pharmaceutical. Our previous work reported the selective hydrogenation of aromatic carboxylic acids over basic N-doped mesoporous carbon supported palladium catalysts [14], these N-doping materials showed high catalytic activity for the selective hydrogenation of aromatic ring. The present paper reports a simple microwave-heating preparation method for biocarbon supported Ni NPs (nanoparticles) catalyst and its application in the ring hydrogenation of benzoic acid under mild conditions. The influence of microwave heating power on the dispersion and morphology of Ni and the benzoic acid hydrogenation is discussed.

2. Experimental

2.1. Preparation of catalysts

All chemicals were purchased from were purchased from Shanghai Aladdin Chemical Co.The 10%Ni/CSC-a catalyst was prepared through conventional impregnation method, as described in our previously published articles [36].

An aqueous solution of $Ni(NO_3)_2{\cdot}6H_2O$ was impregnated onto various carbon supports like coconut shell charcoal (CSC), activated carbon (AC) and graphite (G). Typically, 1.0 g carbon was dispersed in 50 mL deionized water consisted of $Ni(NO_3)_2{\cdot}6H_2O$ (0.493 g). Then, the resulting mixture was heated to 90 °C while stirring and heating in microwave reactor. Afterwards, the composite catalyst precursors were obtained by evaporating the water under rotary evaporator at 70 °C and dried in a vacuum oven at 120 °C for 8 h, followed by reduction with H_2 at 400 °C (with a rate of 5 °C/min H_2) for 3 h in a tubular reactor. The resultant catalyst was designated as 10%Ni/CSC-b, 10%Ni/AC-b, 10%Ni/G-b. Other two different samples with the same nominal loading of 10 wt% (weight percent) were prepared by using SiO_2 and Al_2O_3 as supports and designated as 10%Ni/SiO_2-b and 10%Ni/Al_2O_3-b.

2.2. Characterizations

X-ray diffraction (XRD) measurements were performed on a Bruker D8A25 diffractometer with Cu Kα radiation. The tube voltage was 30 kV, and the current was 25 mA. The XRD diffraction patterns were taken in a range of 5–65° 2θ. Quantachrome iQ-MP was used to determine N_2 adsorption–desorption properties of the samples. The specific surface area was calculated by using the Brunauer–Emmett–Teller (BET) method, and the pore size distributions were measured by using Barrett–Joyner–Halenda (BJH) analysis from the desorption branch of the isotherms. The Scanning Electron Microscope (SEM) has been used a JEOL JSM-6510A to detect the morphology and size of crystals. Transmission electron microscope (TEM) (JEOL-135 2010F, operating at 200 kV) was used to investigate morphology and size of the particles. The samples for TEM were prepared by dispersing the material in ethanol and drop-drying onto a Formvar resin coated copper grid. The X-ray photoelectron spectroscopy (XPS) analysis was performed on a Perkin-Elmer PHI ESCA system with 0.1 eV per step for detail scan, and the X-ray source was standard Mg anode at 12 kV and 300 W. The TPR (temperature programmed H_2 reduction) experiments were performed with 10 vol% hydrogen in N_2 (50 mL/min) at a heating rate of 10 °C/min, the hydrogen consumption being measured by a TCD detector. All TPR profiles were normalized for the same catalyst mass.

2.3. Catalytic tests

Hydrogenation of benzoic acid and derivatives was carried out using the as-prepared 10%Ni/CSC-a as the catalyst. Other nickel supported catalysts were also applied in the hydrogenation of benzoic acid for comparison. In a typical process, 4 mmol benzoic acid and a certain amount of catalyst were put into a 100 mL stainless autoclave, and 10 mL solvent was employed as green solvent. The hydrogenation of benzoic acid was carried out at desired temperature with magnetic stirring at a speed of 1000 rpm. After reaction, the filtrate was analyzed by GC-FID with a 30 m capillary column (Rtx@-5). The catalyst was recovered by centrifugation and then washed several times with THF. The separated catalyst was washed several times with THF and dried overnight in an vacuum oven at 80 °C for use in the next run.

3. Results and discussion

3.1. Structural characterizations

Fig. S1 presents the XRD patterns of the samples with different Ni contents. The characteristic peaks of CSC (2θ = 23.3°) and Ni metal (2θ = 45.3, 51.5 and 76.2°) are observed for all the Ni/carbon catalysts with the carrier is CSC, AC and G, respectively, in which three peaks at 45.3°, 51.5° and 76.2° are attributed to [111], [200] and [220] diffraction peaks of Ni. The micropore structure of the 10%Ni/CSC catalysts were identified by nitrogen adsorption/desorption isotherms (Fig. 1). The results clearly show BET surface area of 10%Ni/CSC-a is 599.6 m^2/g, smaller than 678.2 m^2/g of 10%Ni/CSC-b (prepared by microwave-heating). The support CSC still retained its microporsity well after the loading of Ni nanoparticle. Table S1 presents the BET surface areas and total pore volumes of various catalysts determined by the BET analysis. Very clearly, the support G and the catalyst 10%Ni/G-b have the smallest BET surface areas and the pore volumes. Both values of the catalyst 10%Ni/AC-b (activated carbon as the support) are the largest.

Usually, SEM is used to determine the particle size and particle morphology of the synthesized sample. The SEM backscattered composition images of the monometallic Ni/carbon samples are given in Fig. 2, inclusive of 10%Ni/CSC-a, 10%Ni/CSC-b, 10%Ni/AC-b and 10%Ni/G-b. Apparently, SEM images of four samples exhibit irregular spherical morphologies, and it is clear that most of the catalyst particles are in good dispersion. TEM images of metal particle size distribution of 10%Ni/CSC-a, 10%Ni/CSC-b, 10%Ni/AC-b and 10%Ni/G-b are shown in Fig. 3. For 10%Ni/CSC-a, a wide particle size distribution is observed and the metal particle size is varied from 6.3 to 39.9 nm with an average value of 13.2 nm (Table 1). The particle sizes of Ni metal supported on AC and G are determined to be 17.7 and 12.7 nm, respectively. For 10%Ni/CSC-b, highly dispersed Ni nanoparticles are found to evolve and distribute throughout the CSC-b. The mean diameter is estimated to be 9.4 nm. This demonstrates that the microwave-heating plays an important role in the dispersion of metallic species over the CSC support.

Fig. 4 shows TEM images of 10%Ni/CSC-b, in which particle size and dispersion on catalysts are affected by microwave-heating power. When the microwave heating power is 400 W, the mean particle size of Ni on 10%Ni/CSC-b is 14.7 nm. As the microwave power increases to 500 W, the 10%Ni/CSC-b shows the presence of uniformly well-dispersed Ni on CSC, and the mean diameter is estimated to be 9.4 nm. The mean particle size of Ni is decreased to 7.9 nm on 10%Ni/CSC-b (600 W). When the catalyst 10%Ni/CSC-b (700 W) is prepared by 700 W microwave-heating power, the mean particle size of Ni nanoparticles on the CSC support is reduced to 7.7 nm with a wide distribution. However, the hydrogenation activity of the catalysts shows that the microwave-heating power of 500 W is optimal for the preparation of the catalyst.

X-ray photoelectron spectroscopy is a convenient method of studying supported nickel catalysts. The reducibility and interactions between metal and support are further studied by H_2-TPR, as

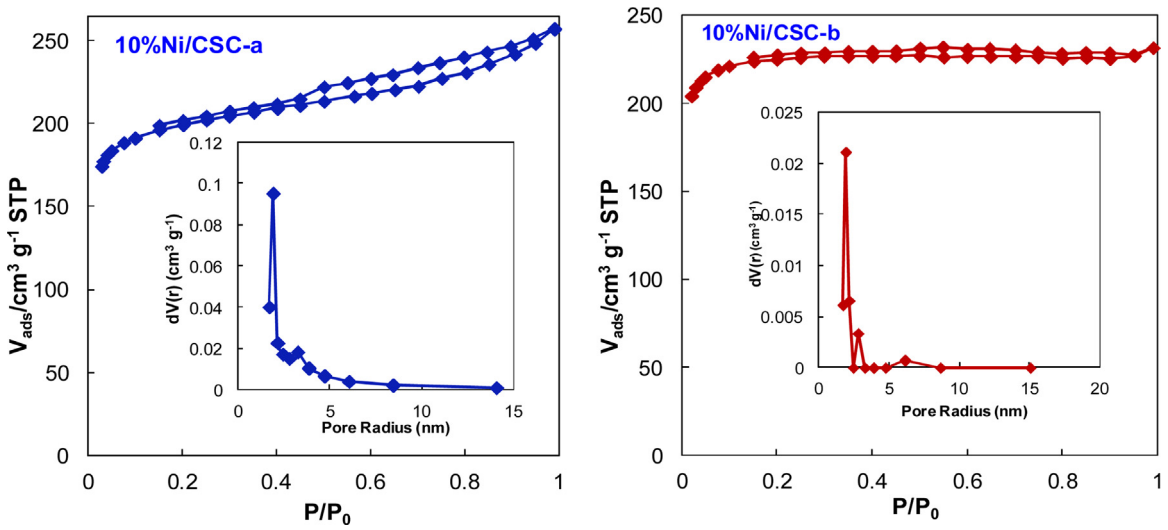

Fig. 1. Nitrogen sorption isotherms and pore size distribution of 10%Ni/CSC catalysts.

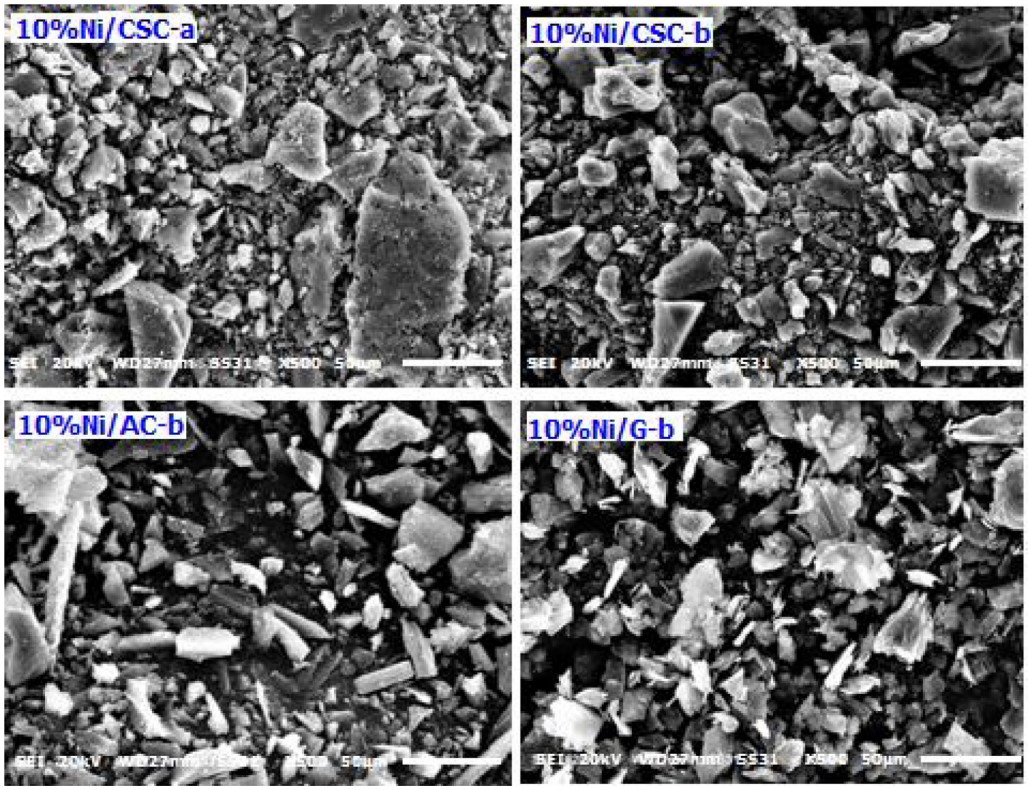

Fig. 2. SEM images of carbon supported Ni catalysts.

Table 1
Physical properties of the supported Ni/carbon materials.

Catalysts	Preparation mode	Particle size (nm)		Relative atomic percentage (%)		
		XRD	TEM	Ni^0	NiO	$Ni(OH)_2$
10%Ni/CSC-a	No microwave-heating	15.5	13.2	9.7	6.9	83.4
10%Ni/CSC-b	Microwave-heating	8.9	9.4	12.4	20.0	67.6

shown in Fig. 5. The metal nickel is characterized by a peak at about 853 eV, and peaks above this energy correspond to Ni^{2+} [37]. The peak at 853 eV corresponding to the Ni^0 is observed for the catalysts, as shown in Fig. 5. The main Ni 2p3/2 peaks for all samples are found to be at 854.2 and 856.0 eV [38], revealing that surface Ni is mainly in the state of NiO and Ni^{2+} ($Ni(OH)_2$). These results show that part of the metallic nickel has been oxidized after the contact of the sample with air [39]. In the case of 10%Ni/CSC-a and 10%Ni/CSC-b, a minor contribution is recorded at a lower binding energy of 853 eV, which can be assigned to Ni in the metallic state.

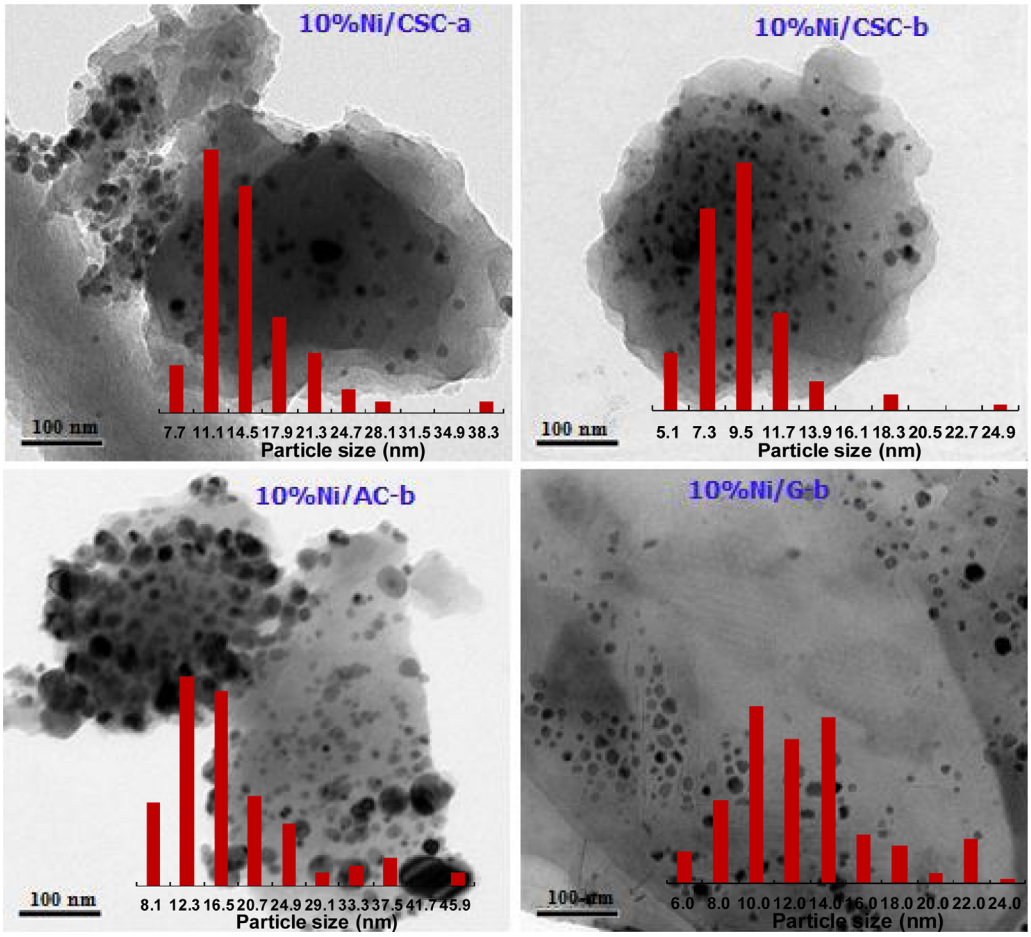

Fig. 3. TEM images of the supported catalysts and size distribution of Ni particles on *x*%Ni/carbon.

For example, the percentage of metallic Ni (Table 1) in 10%Ni/CSC-b is 12.4%, which is higher than that of 10%Ni/CSC-a (9.7%).

TPR is a favorable technique for studying supported nickel catalysts. Fig. 6 shows the H_2-TPR profiles of the supported Ni catalysts, a "NiO"-like defect phase, produced by oxidation of supported metal nickel, is reduced in the temperature interval of 250 – 450 °C. Thus, in the TPR profile of 10%Ni/CSC-a three TPR signals at 287, 316 and 336 °C are ascribable to the reduction of NiO particles to metal Ni^0 without interaction with the support (at 287 and 316 °C), and to the reduction of Ni^{2+} with medium interaction (at 336 °C) [40,41]. This evidences some inhomogeneity of supported nickel. According to data from the literature [42–44], the TPR peaks are due to reduction of the supported "NiO"-like phase. There are different reduction peaks for the resulting 10%Ni/CSC-b in four stages with the main signals at 267, 293, 321 and 393 °C, in which the first reduction peak appears at lower temperature than the other three samples. The appearance of the peak at high temperature of 393 °C, with other two peaks at 293 and 321 °C, is attributable to the reduction of Ni^{2+} with strong interaction. When the carrier is replaced by AC, the H_2-TPR profile of 10%Ni/AC-b shows that the reduction of nickel species on AC occurs in five stages with maximal signals at 276, 288, 313, 330 and 409 °C. However, the H_2-TPR profile of 10%Ni/G-b has only two maximal signals at 301 and 325 °C.

3.2. Catalytic hydrogenation of BA to CCA

For the hydrogenation of BA to CCA, the activity of different Ni catalysts is compared in Table 2. Over 10%Ni/CSC-a, the hydrogenation affords only 35.9 mol% conversion of BA with 100% selectivity of CCA (entry 1). As compared with 10%Ni/CSC-a, the catalytic activity of 10%Ni/CSC-b increases to 86.2 mol% conversion of BA with 100% selectivity of CCA (entry 2). The 10%Ni/AC-b catalyst shows a poor activity with only 40.8 mol% conversion of BA (entry 3). Other heterogeneous Ni-based catalysts inclusive of 10%Ni/G-b, 10%Ni/SiO_2-b and 10%Ni/Al_2O_3-b (entries 4–6) achieve a poor hydrogenation activity <34 mol% under the same reaction conditions.

Nickel loading changes the dispersive state of Ni species across carbon carrier, which will further affect the reaction network in steam reforming, since the Ni species is the active site for those reactions [45,46]. Benzoic acid conversion and product distribution are presented in Fig. 7. As shown in Fig. 7, nickel loading significantly affects the catalytic activity of the catalyst. The blank catalyst shows no hydrogenation activity. The presence of 5 or 7 wt.% nickel loading on CSC-b promotes the catalytic activity, but the promotion is limited, due to the lack of enough active sites for hydrogenation. Further increasing the nickel loading to 10 or 15 wt.% remarkably improves the hydrogenation activity, the conversion of BA is also improved from 67.0 to 86.2 mol% or 86.5 mol%. As for Ni (≥20 wt.%)/CSC catalysts, the conversion of BA is decreased to 70.2 mol%. This result indicates that the amount of Ni loading lies in an appropriate range, more and less metal loading is inappropriate. Encouragingly, the selectivity of CCA has been maintained at the level of 100%.

The microwave-heating power used in the preparation of catalyst also has some impact on the catalytic activity of the hydrogenation catalyst, as shown in Fig. 8. When microwave power is 400 W, there is 67.9 mol% conversion of BA, which is signifi-

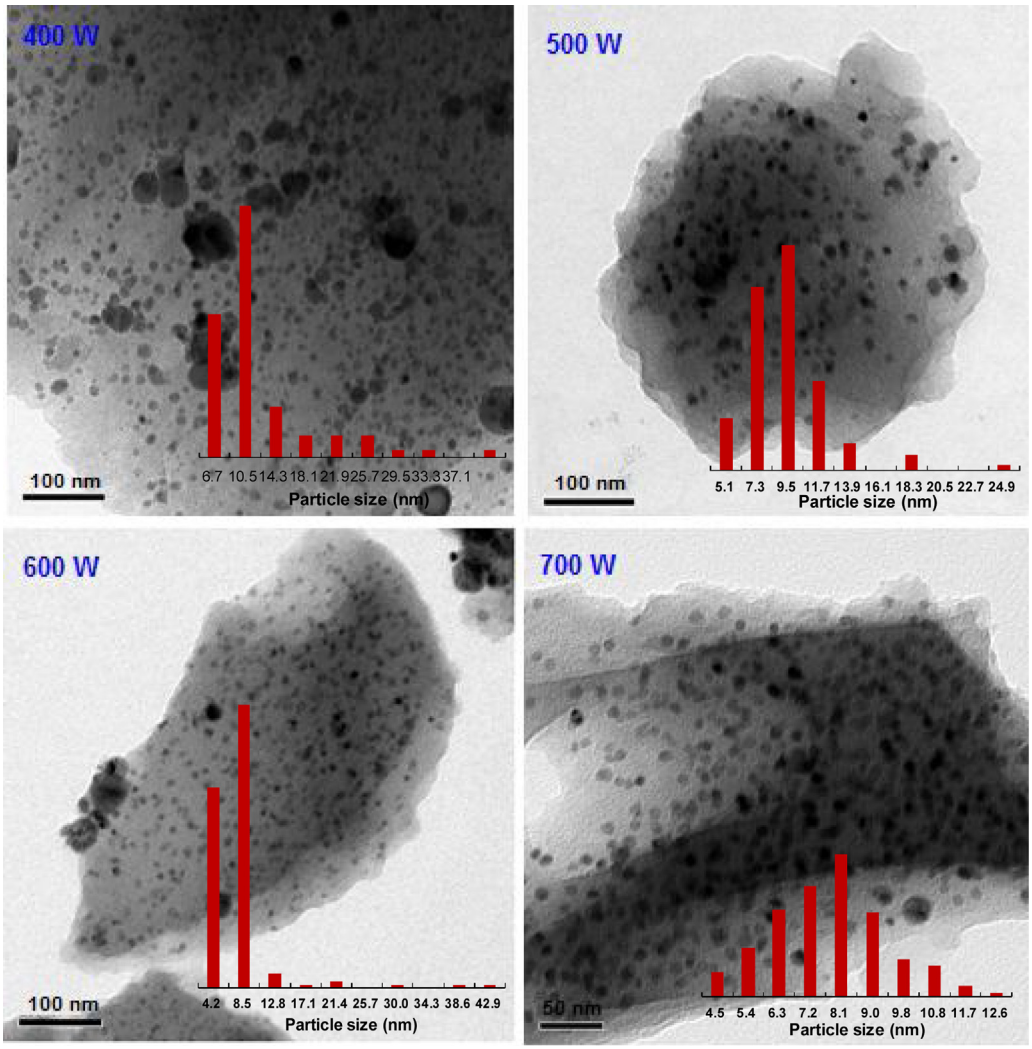

Fig. 4. TEM images of the 10%Ni/CSC-b catalysts prepared using different microwave-heating powers.

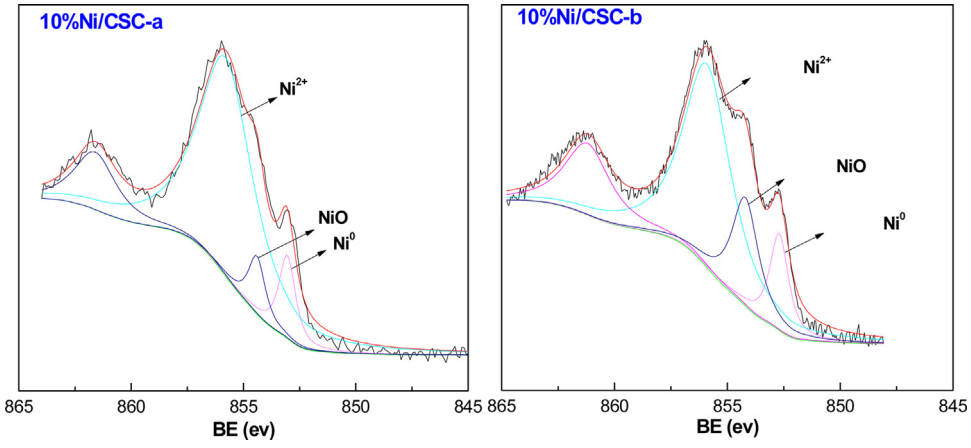

Fig. 5. Ni2p XPS spectra of 10%Ni/CSC-a and 10%Ni/CSC-b.

cantly lower than 86.2 mol% conversion on the catalyst prepared by the microwave power of 500 W. With a further increase of the microwave power to 700 W, the conversion of BA is slowly decreased to 78.5 mol%. This shows that suitable microwave power is very conducive for improving the catalytic activity of the catalyst. TEM images (Fig. 4) and XPS spectra (Fig. S2) also show the distribution of different catalyst components and particles treated by different microwave powers, in agreement with different hydrogenation activities.

The selective hydrogenation of aromatic compounds with both aromatic rings and other reducible groups usually requires severe conditions over non-noble metal catalysts. The chemoselective

Table 2
Hydrogenation of BA over different catalysts.[a]

Entry	Catalyst	T (°C)	Conversion (mol%)	Selectivity (%)	
				CCA	Others
1	10%Ni/CSC-a	200	35.9	100	0
2	10%Ni/CSC-b	200	86.2	100	0
3	10%Ni/AC-b	200	40.8	100	0
4	10%Ni/G-b	200	33.8	100	0
5	10%Ni/SiO_2-b	200	32.5	100	0
6	10%Ni/Al_2O_3-b	200	18.0	100	0

[a] Reaction conditions: 4.0 mmol BA, 100 mg catalyst, 10 mL THF, 3.0 MPa H_2, 8 h.

Table 3
Hydrogenation of BA in different solvents.[a]

Entry	Catalyst	Solvent	T (°C)	Conversion (mol%)	Selectivity (%)	
					CCA	Other
1	10%Ni/CSC-b	THF	200	86.2	100	0
2		Cyclohexane	200	35.6	100	0
3		Dioxane	200	16.2	100	0
4		Ethanol	200	10.1	100	0
5		Cyclohexanol	200	13.9	100	0
6		Water	200	54.2	100	0

[a] Reaction conditions: 4.0 mmol BA, 100 mg catalyst, 10 mL solvent, 3.0 MPa H_2, 8 h.

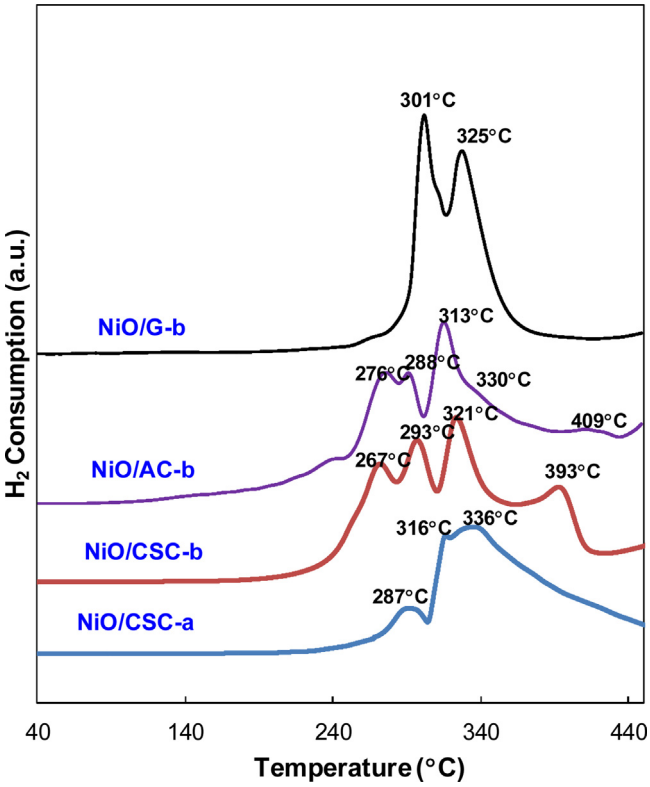

Fig. 6. Effect of Ni content on H_2-TPR profiles of NiO/CSC.

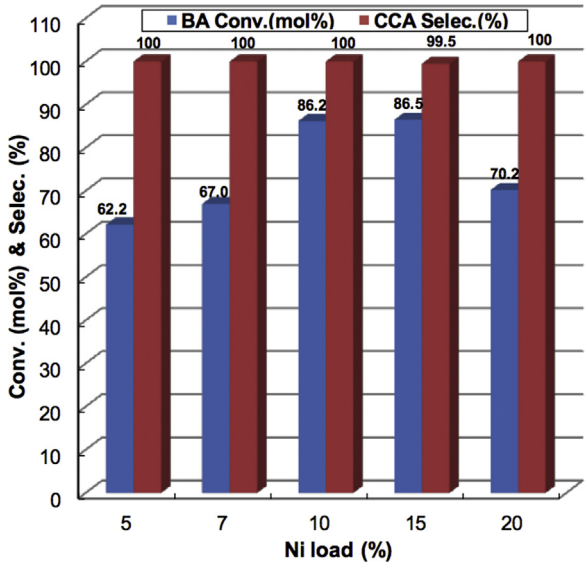

Fig. 7. Catalytic activity of *x*%Ni/CSC-b catalysts. (Conditions: 4.0 mmol BA, 100 mg catalyst, 10 mL THF, 3.0 MPa H_2, 200 °C, 8 h.).

hydrogenation of BA was therefore studied in a series of solvents over 10%Ni/CSC-b to investigate the effect of solvents on the activity, and the results are shown in Table 3. As summarized in Table 3, among these solvents, cyclohexane, dioxane, ethanol and cyclohexanol are unfavorable for this reaction (entries 2–5). Although a certain amount of CCA is obtained in ethanol (entry 4), the BA conversion is only 10.1 mol%. When water is employed as the solvent (entry 6), the conversion of BA reaches 54.2 mol% at 200 °C for 8 h under 3.0 MPa of H_2. When THF is employed as the solvent (entry 1), the conversion of BA is rapidly increased to 86.2%.

The effect of catalyst amount on the conversion and selectivity is illustrated in Fig. 9. Reactions were carried out to find the minimum weight of the catalyst required to achieve the necessary conversion. The BA conversion increased with catalyst concentration from 25 to 100 mg, the conversion of BA is rapidly increased from 1.9 to 86.2 mol%, while the selectivity of CCA is maintained at 100%. As the amount of the catalyst increases, more surface area is available for the hydrogenation reaction to take place. The initial conversion rate of BA has a proportional increase with the catalyst amount. As the catalyst amount increased from 100 to 150 mg, the conversion of BA is slightly increased from 86.2 to 86.8 mol%.

The temperature has a significant effect on the conversion of BA. Reactions were carried out at 160, 180, 190, 200, and 220 °C and at a pressure of 3.0 MPa of hydrogen in the presence of 10%Ni/CSC-b catalyst. Fig.S3 shows the effect of temperature on the hydrogenation of BA. As the reaction temperature is increased from 160 to 180 °C, the conversion of BA is increased from 11.5 to 35.8 mol%. As

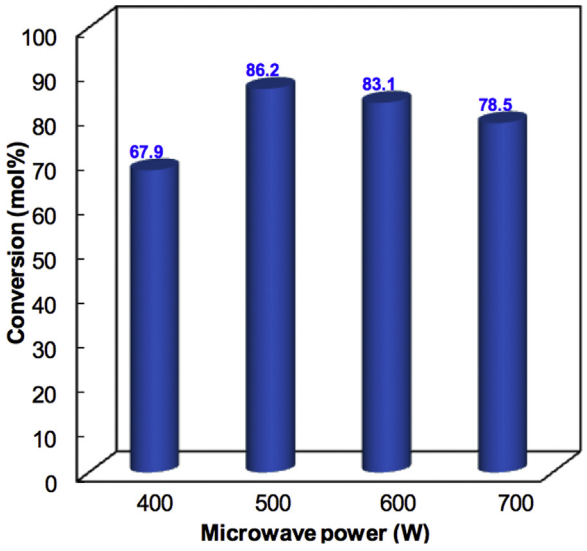

Fig. 8. Effect of the microwave power on the hydrogenation. (Conditions: 4.0 mmol BA, catalyst 10%Ni/CSC-b, 10 mL THF, 3.0 MPa H_2, 200 °C, 8 h.).

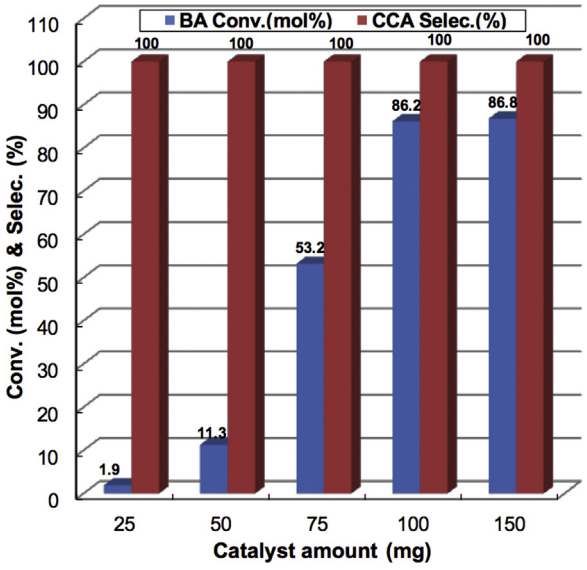

Fig. 9. Effect of the catalyst amount on the hydrogenation. (Conditions: 4.0 mmol BA, catalyst 10%Ni/CSC-b, 10 mL THF, 3.0 MPa H_2, 200 °C, 8 h.).

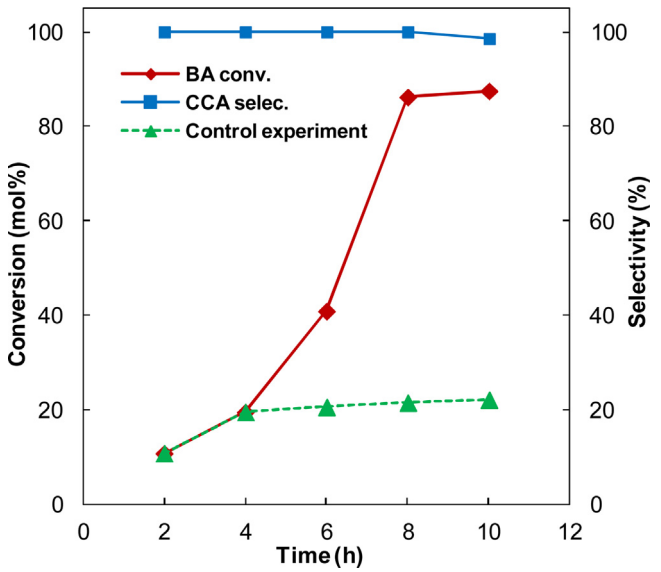

Fig. 10. Effect of the reaction time on the hydrogenation. (Conditions: 4.0 mmol BA, 100 mg catalyst (10%Ni/CSC-b), 10 mL THF, 3.0 MPa H_2, 200 °C.).

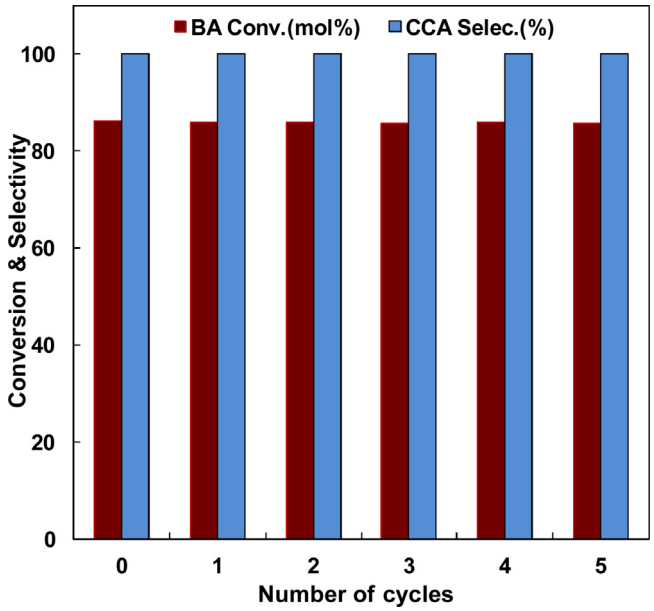

Fig. 11. Recycling results of the catalyst 10%Ni/CSC-b. (Conditions: 4.0 mmol BA, 100 mg catalyst (10%Ni/CSC-b), 10 mL THF, 3.0 MPa H_2, 200 °C.).

the reaction temperatures is increased from 180 to 200, the BA is rapidly increased from 35.8 to 86.2 mol%. With a continuous lift of reaction temperature to 220 °C, the conversion of BA is changed a little (86.8 mol%), but the selectivity of the product CCA is slightly reduced to 98.2%.

Fig. 10 gives the effect of reaction time concerning the change of conversion in selective hydrogenation of BA as a function of time. In the case of the 10%Ni/CSC-b, within 2 h of reaction time, the conversion increased slowly (the conversion of BA is only 10.8 mol%.). At the reaction time of 8 h, the conversion increased sharply to 86.2 mol%, while the selectivity maintained at 100%. As prolong the reaction time to 10 h, the conversion increased slowly (87.5 mol%). Comparatively, the selectivity of product CCA is slightly decreased from 100 to 98.2%, probably due to the increase of side product cyclohexyl-methanol. The yield of CCA reaches the maximum of 86.2 mol% in 8 h, which is the optimal time. On the basis of these data, control experiments have been carried out under identical reaction conditions, but in the absence of any metal catalysts [47]. As shown in Fig. 10, after the hydrogenation reaction is initially conducted for 4 h, the conversion of BA reaches 19.5 mol%. Then, the solid catalyst is filtered off and the reaction is continued for another 6 h. In the absence of metal catalyst, however, a small increment of 2.6 mol% conversion of BA could be observed, which further confirms the characteristics of heterogeneous catalysis.

The 10%Ni/CSC-b catalyst can be easily separated by centrifugation for five recycles without obvious loss of activity or CCA selectivity (Fig. 11). For example, the 10%Ni/CSC-b catalyst at the fifth recycle has 85.7 mol% conversion of BA, still comparable to the fresh catalyst (86.2 mol%). For the first recycle, ICP analyses of the reaction mixture and the used catalyst did not detect the leaching of Ni from CSC. The estimated Ni content remained just about the same as the fresh catalyst. For the latter four recycles, still no leaching of Ni was detected. This study further reveals the recyclable stability of the active catalyst 10%Ni/CSC-b for the titled reaction.

Table 4
Hydrogenation of benzoic acid derivatives over 10%Ni/CSC.[a]

Entry	Catalyst	Substrate	Product	Conversion (mol%)	Selectivity(%)
1	10%Ni/CSC-b	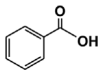	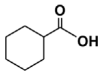	86.2	100
2		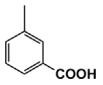	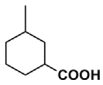	72.8	100
3		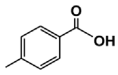	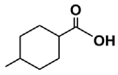	71.3	100
4		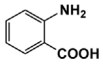	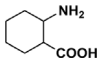	52.3	100
5		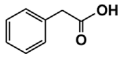	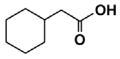	55.3	100
6		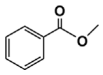	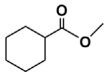	38.6	100

[a] Reaction conditions: 4.0 mmol substrate, 100 mg catalyst, 10 mL THF, 3.0 MPa H_2, 200 °C, 8 h.

Also, 10%Ni/CSC-b catalyst showed good activity in the hydrogenation of benzoic acid derivatives (Table 4). Benzoic acids with an electron-donating group on the ring of (*meta*-methylbenzoic acid and *para*-methylbenzoic acid, entry 2 and 3) afford slightly lower conversions (72.8 and 71.3 mol%) compared to benzoic acid. For the example of anthranilic acid (entry 4), a relatively low conversion (52.3 mol%) is obtained. The hydrogenation of phenylacetic acid reaches 55.3 mol% conversion in 8 h (entry 5). Furthermore, 38.6 mol% conversion of methyl benzoate (entry 6) is obtained over 10%Ni/CSC-b in 8 h.

4. Conclusion

Metallic Ni nanoparticles have been highly dispersed over CSC, AC, G, Al_2O_3 and SiO_2 by an efficient strategy of microwave-assisted mode. By microwave-assisted mode, a narrow distribution of Ni nanoparticle size centred at around 9.4 nm can be obtained. The robust 10%Ni/CSC-b catalyst shows high catalytic activity and excellent reusability in the hydrogenation of aromatic acid compounds, such as benzoic acid or other aromatic acids. The excellent catalytic activity is attributed to the co-effect of the support and the microwave-heating power, which provides suitable disperse condition of metallic active centres. The effect of the support, the Ni loading content, the microwave power was deeply investigated at mild reaction conditions. In addition, the present catalyst showed good stability and could be reused five times without loss of product yields.

Acknowledgements

The authors thank financial support from the National Natural Science Foundation of China (21503074, 21673069, 21603066, 21571055), the Hubei Province Natural Science Fund for Creative Research Groups (2014CFA015) and the Hubei Provincial Outstanding Youth Foundation of China (2016CFA040).

Appendix A. Supplementary data

Supplementary data associated with this article can be found, in the online version, at http://dx.doi.org/10.1016/j.mcat.2017.10.015.

References

[1] M. Takahashi, T. Imaoka, Y. Hongo, K. Yamamoto, Angew. Chem. Int. Ed. 52 (2013) 7419.
[2] G. Vile, B. Bridier, J. Wichert, J. Perez-Ramirez, Angew. Chem. Int. Ed. 51 (2012) 8620.
[3] S. Cao, J.R. Monnier, C.T. Williams, W.J. Diao, J.R. Regalbuto, J. Catal. 326 (2015) 69.
[4] I. Nakamula, Y. Yamanoi, T. Imaoka, K. Yamamoto, H. Nishihara, Angew. Chem. Int. Ed. 50 (2011) 5830.
[5] J. Scalbert, F.C. Meunier, C. Daniel, Y. Schuurman, Phys. Chem. Chem. Phys. 14 (2012) 2159.
[6] A. Seidel, Cytoskeleton, John Wiley, Hoboken, N.J, 2007, pp. 590.
[7] D.G. Cheng, M.B. Chong, F.Q. Chen, X.L. Zhan, Catal. Lett. 120 (2008) 82.
[8] Y. Sakata, C.A. Tol-Koutstaal, V. Ponecz, J. Catal. 169 (1997) 13.
[9] W.F. HoÈlderich, J. Tjoe, Appl. Catal. A: Gen. 184 (1999) 257.
[10] T. Yokoyama, N. Yamagata, Appl. Catal. A: Gen. 221 (2001) 227.
[11] B. Nair, Int. J. Toxicol. 20 (2001) 23.
[12] T.J. Korstanje, J.I. Vlugt, C.J. Elsevier, B. Bruin, Science (2015) 298.
[13] N. Perret, X.D. Wang, J.J. Delgado, G. Blanco, X.W. Chen, C.M. Olmos, S. Bernal, M.A. Keane, J. Catal. 317 (2014) 114.
[14] H.Z. Jiang, X.L. Yu, R.F. Nie, X.H. Lu, D. Zhou, Q.H. Xia, Appl. Catal. A: Gen. 520 (2016) 73.
[15] X. Xu, M.H. Tang, M.M. Li, H.R. Li, Y. Wang, ACS Catal. 4 (2014) 3132.
[16] H.J. Wang, F.Y. Zhao, Int. J. Mol. Sci. 8 (2007) 628.
[17] G.Y. Bai, X. Wen, Z. Zhao, F. Li, H.X. Dong, M. Qiu, Ind. Eng. Chem. Res. 52 (2013) 2266.
[18] H. Shinkai, K. Toi, I. Kumashiro, Y. Seto, M. Fukuma, K. Dan, S. Toyoshima, J. Med. Chem. 31 (1988) 2092.
[19] H. Shinkai, M. Nishikawa, Y. Sato, K. Toi, I. Kumashiro, Y. Seto, M. Fukuma, K. Dan, S. Toyoshima, J. Med. Chem. 32 (1989) 1436.
[20] B.S. Moore, H.J. Cho, R. Casati, E. Kennedy, K.A. Reynolds, U. Mocek, J.M. Beale, H.G. Floss, J. Am. Chem. Soc. 115 (1993) 5254.
[21] D.Y. Murzin, Kinet. Catal. 32 (1991) 1318.
[22] G.Y. Bai, X. Wen, Z. Zhao, F. Li, H.X. Dong, M.D. Qiu, Ind. Eng. Chem. Res. 52 (2013) 2266.
[23] H.J. Wang, F.Y. Zhao, Int. J. Mol. Sci. 8 (2007) 628.
[24] T. Yokoyama, N. Yamagata, Appl. Catal. A: Gen. 221 (2001) 227.
[25] B.N. Zong, X.X. Zhang, M.H. Qiao, AIChE J. 55 (2009) 192.
[26] R. Raja, T. Khimyak, J.M. Thomas, S. Hermans, B.F. Johnson, Angew. Chem. Int. Ed. 40 (2001) 4638.
[27] Z.Q. Guo, L. Hu, H.H. Yu, X.Q. Cao, H.W. Gu, RSC Adv. 2 (2012) 3477.
[28] V. Polshettiwar, M.N. Nadagouda, R.S. Varma, Chem. Commun. (2008) 6318.
[29] R.F. Nie, X.L. Peng, H.F. Zhang, X.L. Yu, X.H. Lu, D. Zhou, Q.H. Xia, Catal. Sci. Technol. 7 (2017) 627.
[30] S.F.J. Hackett, R.M. Brydson, M.H. Gass, I. Harvey, A.D. Newman, K. Wilson, A.F. Lee, Angew. Chem. Int. Ed. 46 (2007) 8593.
[31] Q.H. Xia, S.C. Shen, J. Song, S. Kawi, K. Hidajat, J. Catal. 219 (2003) 74.
[32] J.A. Anderson, A. Athawale, F.E. Imrie, F.M. Mkenna, A. Mcue, D. Molyneux, K. Power, M. Shand, R.P.K. Wells, J. Catal. 270 (2010) 9.
[33] R. Nie, J. Wang, L. Wang, Y. Qin, P. Chen, Z. Hou, Carbon 50 (2012) 586.
[34] J. Wang, G. Fan, F. Li, Catal. Sci. Technol. 3 (2013) 982.
[35] R.F. Nie, H.Z. Jiang, X.H. Lu, D. Zhou, Q.H. Xia, Catal. Sci. Technol. 6 (2016) 1913.
[36] X.H. Lu, Y. Chen, Z.S. Zhao, H. Deng, D. Zhou, C.C. Wei, R.F. Nie, Q.H. Xia, RSC Adv. 6 (2016) 15354.

[37] A.G. Sault, J. Catal. 156 (1995) 154.
[38] P. Prietoa, V. Nistor, K. Nouneh, M. Oyama, M.A. Lefdil, R. Diaz, Appl. Surf. Sci. 258 (2012) 8807.
[39] Z.Y. Hou, Q. Yokota, T. Tanaka, T. Yashima, Appl. Catal. A: Gen. 253 (2003) 381.
[40] X.H. Lu, X.L. Wei, D. Zhou, H.Z. Jiang, Y.W. Sun, Q.H. Xia, J. Mol. Catal. A: Chem. 396 (2015) 196.
[41] R.K. Sharath, G.S. Boris, V.S. Guggilla, V.R.C. Komandur, C. Abraham, J. Catal. 242 (2006) 319.
[42] P. Burattin, M. Che, C. Louis, J. Phys. Chem. B 101 (1997) 7060.
[43] K. Hadjiivanov, M. Mihaylov, D. Klissurski, P. Stefanov, N. Abadjieva, E. Vassileva, L. Mintchevz, J. Catal. 185 (1999) 314.
[44] M. Che, Z.X. Cheng, C. Louis, J. Am. Chem. Soc. 117 (1995) 2008.
[45] S. Mingyong, E.N. Alan, A. John, J. Catal. 231 (2005) 223.
[46] A. Saadi, R. Merabti, Z. Rassoul, M.M. Bettahar, J. Mol. Catal. A: Chem. 253 (2006) 79.
[47] D. Zhou, B. Tang, X.H. Lu, X.L. Wei, K. Li, Q.H. Xia, Catal. Commun. 45 (2014) 124.